ISTITUTO NAZIONALE DI FISICA NUCLEARE

Sezione di Lecce

INFN/TC–95/06
18 Gennaio 1995

A. Beloglazov, M. Martino, V. Nassini:

HIGH BRIGHTNESS ELECTRON BEAMS INDUCED BY EXCIMER LASERS ON METAL TARGETS

PACS: 29.25.B

SIS–Pubblicazioni
dei Laboratori Nazionali di Frascati

INFN - Istituto Nazionale di Fisica Nucleare
Sezione di Lecce

INFN/TC-95/06
18 Gennaio 1995

HIGH BRIGHTNESS ELECTRON BEAMS INDUCED BY EXCIMER LASERS ON METAL TARGETS

A. Beloglazov*, M. Martino, V. Nassini:

University of Lecce, Department of Physics
National Institute for Nuclear Physics of Lecce, via Arnesano, 73100 Lecce, Italy

* Institute of General Physics, Moscow, Russia

Abstract

This work reports the experimental results relative to electron beam emittance and current photo-extracted from Aluminium, Zinc and Copper targets utilising two excimer lasers of different wavelengths, 308 nm (XeCl) and 222 nm (KrCl). The maximum laser energies utilised were limited by the plasma density on the cathode that short-circuits the diode gap. The output current was higher with KrCl laser than with the XeCl laser for the three metals used and the lower emittance was obtained with the XeCl laser. These results can be ascribed mainly to the difference between laser photon energies and the target work functions. At 20 kV of acceleration voltage, a computer simulation of a space-charge limited electron beam resulted in a total current of 200 mA and the normalised emittance of 20 π mm mrad. The maximum extracted current, 1.03 A, was obtained with Cu targets at 20 kV of accelerating voltage. The output current for large anode-cathode distance was higher than that predicted by the Child-Langmuir law while for small one the current was lower than that theoretical. This behaviour is attributed to the plasma formation on the cathode during the laser action. In fact, during the laser irradiation, a positive pulse of about 1 V at a distance of a few tens of μm from the cathode was measured by means of a Langmuir-like probe. This plasma electric field modifies the space-charge conditions and as a consequence it increases the total current particularly at large anode-cathode distance.

1. INTRODUCTION

The new electron accelerators need high brightness electron beam injectors in order to increase the beam luminosity. These devices can be realised using RF photocathode guns which have confirmed the possibility of getting emittances very lower than those provided by thermionic cathodes [1]. In particular, metal photocathodes seem to be very promising especially when excimer lasers are used to irradiate their surface [2] and they seem also to provide beam emittances much lower than those provided by thermionic cathodes [3].

Excimer lasers allow the application of one-photon photoelectric processes even with metal targets because of their high photon energy which is comparable to the metal work function. This condition is interesting for extracting electron beam of low emittance, in spite of space charge effects and target increasing temperature degrade the beam quality[3-5].

So it is of most importance to investigate the optimum conditions in order to get high brightness electron beams with different lasers and metal targets. The emittance due to the potential distribution and to the space charge effects can be easily calculated by computer simulation while the experimental values take into consideration the emittance due to the source quality too. Recently, it has been supposed that a plasma is formed on the target surface which modifies strongly the experimental values in respect of the theoretical ones [6,7].

We report here on the output current and beam emittance experimental results for three different metals, Al, Zn and Cu, whose work functions are 4.2, 3.9 and 4.5 eV, irradiated with two different excimer lasers: the XeCl (λ=308 nm) and the KrCl (λ=222 nm) ones. Their photon energies are 4.02 eV and 5.6 eV respectively.

2. THEORY

The Richardson equations which govern the electron extraction for XeCl and KrCl lasers are [7,8]:

$$^{Al}J_{308} = {}^{Al}a_{308}\ T^2 I \exp[(4.02 - {}^{Al}\phi)/kT] \quad (1)$$

$$^{Al}J_{222} = {}^{Al}a_{222}\ I(5.6 - {}^{Al}\phi)^2/2k^2 \quad (2)$$

$$^{Zn}J_{308} = {}^{Zn}a_{308}\ I\ (4.02 - {}^{Zn}\phi)^2/2k^2 \quad (3)$$

$$^{Zn}J_{222} = {}^{Zn}a_{222}\ I\ (5.6 - {}^{Zn}\phi)^2/2k^2 \quad (4)$$

$$^{Cu}J_{308} = {}^{Cu}a_{308}\ T^2 I \exp[(4.02 - {}^{Cu}\phi)/kT] \quad (5)$$

$$^{Cu}J_{222} = {}^{Cu}a_{222}\ I(5.6 - {}^{Cu}\phi)^2/2k^2 \quad (6)$$

where a_{308} and a_{222} are the Richardson coefficients respectively for XeCl and KrCl laser, I is the laser intensity, T is the target temperature and k is the Boltzmann constant. These

equations are applicable for one-photon processes. The value of the temperature has to be calculated by heat diffusion equation, metal physical-chemical properties and laser energy density. The temperature behaviour is governed by following formula [9]:

$$T = T_o + C \int_0^{\infty} I(t)\, u(t-t')\, t'^{1/2}\, dt' \tag{7}$$

where T_o is the room temperature, C is a constant dependent on the target material and u(t-t') is the Heaviside function.

The theoretical current in space charge dominated regime is governed by the Child-Langmuir law:

$$I = p\, V^{3/2} \tag{8}$$

where p is the perveance in units of $AV^{-3/2}$ and V is the applied potential.

The normalised emittance upper limit in the plane of incidence of electron extracted can be evaluated by the following formula [3, 10]

$$\varepsilon_o = r\, \Delta\phi/\pi \tag{9}$$

where r is the spot radius and $\Delta\phi$ is the angular divergence.

The normalised transverse beam emittance is

$$\varepsilon_n = \varepsilon_o\, \beta\gamma \tag{10}$$

where β and γ are the relativistic parameters, $\beta = v/c$ with v the speed of the electrons and $\gamma = (1-\beta)^{-1/2}$. The normalised peak brightness of the beam is defined as [10,11]:

$$B_n = I/\varepsilon_n^2 \tag{11}$$

In order to explain the experimental results, we utilised the EGUN simulation code. The values of output current and emittance have been calculated under space-charge regime and aimed measurements of the output current as a function of the anode-cathode distance have been done experimentally.

3. EXPERIMENTAL SET-UP

Fig. 1 shows the acceleration chamber having two symmetric quartz windows and an array of small Faraday cups in front of the cathode. Each cup is 9 mm in diameter and 11.5 mm

distant from each other. All cups are placed into the grounded flange by an insulator and connected to a 50 Ω BNC. In this way, the cups are able to measure only the electron beam current and to prevent the electromagnetic noise.

An HV power supplier fed the cathode (T). The accelerating voltage can vary up to 20 kV. A Rogowski coil (R) and an insulator ring (I) connected the cathode holder to the chamber. The laser beam was focused on the cathode by a 30 cm focal length lens at a grazing incident angle of 70°. The chamber was evacuated by a turbo-molecular pump down to 10^{-7} Torr.

Fig. 2 shows the experimental set-up. The target support was connected to the HV supplier by a 50 Ω coaxial cable, as shows Fig. 2. Its capacitance (~ 100 pF/m) was able to store a charge concentration sufficient to feed the target during the emission and so we did not use buffer capacitors.

The laser device used in this experimental work was described in previous paper [5]. It is very compact owing to the preionization system which is fed by the same electric circuit employed to charge the laser capacitors. Its maximum output energy was higher than 100 mJ but, with neutral density filters, only a small percentage was used in this experiment.

In order to reduce the thermionic emission and to avoid the short-circuit due to plasma formation on the cathode, mechanically polished mirror-like samples having a high reflectivity and low laser energies were used.

The laser spot dimension on the cathode was 2 mm in diameter and the laser energies were chosen in order to achieve the maximum electron intensity without plasma emission which could short-circuit the diode gap. A Dove prism was used to turn the beam of large horizontal divergence by 90°.

In the experiments, two digitising oscilloscopes, a Tek. TDS 540 (1Gs/s) and a Tek. TDS 620 (2GS/s), recorded the waveforms. The electron current signals and the time evolution of the laser beam were detected by a fast Rogowski coil previously described [12], having an attenuation factor of 14.8 A/V and a fast UV photodiode Hamamatsu R1328 U-02

4. EXPERIMENTAL RESULTS

In this section we report on the experimental results obtained with the Al, Zn and Cu metals illumined by 308 and 222 nm wavelength light.

4.1 Al experimental data:

Fig. 3 shows the waveform of 308 nm laser intensity (a), the Rogowski coil and the Faraday cup responses (b) at 5.6 mJ laser energy and 20 kV of accelerating voltage. Only the cups #-1, #0 and #1 picked up the signals. The Rogowski coil current and the Faraday cups

signals have a time duration higher than that of the laser pulse. This behaviour is due to the used laser power and its shape. In particular, it was demonstrated [2] that the lengthening of the current pulse is often due to the target temperature evolution calculated by Eq. (7). It has been proved that for pulse laser used in this work the maximum temperature has formed at the end of the laser pulse and for the cases in which the Eq. (1) is applicable a consistent electron emission is observed in this period [7].

Indeed the total current measured by Rogowski coil, I_t, and the current measured with different cups have different waveform. In particular the current measured with the central cup presents the largest width and it is more than three times larger than the laser pulse. This behaviour can be also ascribed to the larger current picked up by the central cup which is more affected by space-charge. At lower accelerating voltage even the cups #2, #-2, #3, #-3 picked up current due to a larger divergent electron beam.

The output current and emittance as a function of the accelerating voltage are shown in Fig. 4. The current increases vs voltage without achieving the saturation regime indicating the beam is space charge dominated. The emittance decreases slightly vs voltage.

The normalised transverse emittance at 20 kV is 24 π mm mrad. The maximum output current was 250 mA. This value is higher than that of the simulation EGUN code which evaluates a maximum output current of 200 mA and a normalised emittance of 22 π mm mrad. Fig. 5 shows the electron trajectories and the equipotential lines simulated by EGUN in our experimental arrangement.

The experimental results obtained with KrCl laser are shown in Fig. 6(a) and 6(b). Fig. 6(a) shows the KrCl laser waveform and the Fig. 6(b) does the total current, I_t, and the Faraday cup currents at 3.8 mJ laser energy and at 20 kV of acceleration voltage. The current measured by Rogowski coil was 960 mA and the shapes of the various current waveforms are different like previously.

In this case current pulses are present on the cups #-2,#-1,#0, #+1, #+2. The largest current measured by central cup presents the largest width while the current measured by more external cups have a width similar to laser one. The largest current width of the central cup is two times larger than the laser one. This lengthening is higher than that observed in previous experiment, and it can not be entirely ascribed to increasing temperature, as can be seen in Eq. (2), but also to a greater space-charge effect due to the higher current particularly on more internal cups.

Fig. 7 shows the output current and their emittance values versus the accelerating voltage.

In order to compare different electron beam sources with the same total current, we performed measurements with a lower KrCl laser energy (0.6 mJ) which produced an output current, at 20 kV, of about 250 mA very nearly to that obtained with the XeCl. The

corresponding results are shown in Fig. 8. The behaviour of output current and emittance was similar to the previous cases although lower current resulted in lower emittance values.

The maximum brightness were 0.43 10^9 A[π m rad]$^{-2}$ and 0.63 10^9 A[π m rad]$^{-2}$ respectively for XeCl and KrCl Laser.

4.2 Zn experimental data:

The laser energies used for Zn experiments were 5.6 mJ with XeCl laser while 5.6 and 0.38 mJ with KrCl. The laser pulse waveforms were very similar to that found with the Al target.

The Fig. 9 shows the output current and emittance as a function of the accelerating voltage for XeCl laser. The total current and the emittance are higher than those obtained with the aluminium. The maximum current was 400 mA and the normalised emittance was 22 π mm mrad.

In Fig. 10 we observe the same parameters using a KrCl laser with 5.6 mJ of energy. The maximum current was 890 mA at 20 kV of accelerating voltage and the relative normalised emittance was 45 π mm mrad.

In Fig. 11, the laser energy was 0.38 mJ and we measured an output current of 400 mA at 20 kV and a normalised emittance of 33 π mm mrad.

We can note that, although the Zn work function is lower than that of the Al, the peak output current was lower.

The output current obtained, irradiating the Zn target with 0.38 mJ of 222 nm laser light, was similar to that obtained with 5.6 mJ of 308 nm light while the emittance value was higher. This behaviour can be ascribed to higher photon energy of KrCl laser which contributes to increase the transverse electrons temperature. At 20 kV the maximum brightness values were 0.57 10^9 A[π m rad]$^{-2}$ and 0.44 10^9 A[π m rad]$^{-2}$ for XeCl and KrCl laser, respectively.

4.3 Cu experimental data:

The laser energies used for Cu experiments were 5.6 mJ with XeCl laser while 5.6 and 1 mJ with KrCl. . The laser pulse waveforms were very similar to that found with the other targets.

Figs. 12 and 13 show the output current and emittance vs accelerating voltage with equal XeCl and KrCl laser energies respectively.

With this target we observed a current pulse of 1030 mA at 20 kV and a normalised emittance of 47 π mm mrad with 5.6 mJ of KrCl laser energy while we had a maximum current of 36 mA and a normalised emittance of 12 π mm mrad with XeCl laser.

The results at 1 mJ KrCl laser are reported in Fig. 14. These results provide emittance values similar to those obtained with XeCl laser.

The maximum brightness were 0.25 10^9 A[π m rad]$^{-2}$ and 0.46 10^9 A[π m rad]$^{-2}$ for XeCl and KrCl laser, respectively.

It is surprising that the highest work function metal has produced the highest current intensity. Surely plasma is produced during the experiment.

4.4 Study of the plasma formation

Specific measurements were done in order to understand the excess of the current in comparison with the theoretical value, investigating the plasma formation on the target during the laser pulse. It short-circuits the anode-cathode gap as the laser energy increases.

We investigated the formation of plasma during the 5.6 mJ XeCl laser action by inserting a probe near the Al cathode with no accelerating voltage. A positive signals of 1 V was measured at a distance of 10 μm from the cathode and it vanished at a distance of a few mm.

Indeed further study was performed with a plane parallel diode arrangement, of known perveance, where the laser spot was 90 mm^2 and the diode gap was variable up to 16 mm. The perveance value was estimated to be 2.34 x 10^{-6} [$AV^{-3/2}$]. Figs. 15 and 16 show the experimental data and the theoretical values of the current for 2 mm and 16 mm diode gap, respectively. It can be noted that for short gap distance the experimental values are lower than theoretical ones while for large gap the experimental values are greater than theoretical ones. The discrepancy for small gap was explained in previous paper [7], where a plasma impedance was present which decreases the applied accelerating voltage during the electron beam propagation.

With large gap this applied voltage decreasing was negligible due to the low total current value and to the limited thickness of the plasma layer which was about 1 mm while the maximum anode-cathode distance was 16 mm in plane parallel arrangement and 105 mm in first set-up. Instead the plasma electric field added to the applied electric field modifying the space-charge conditions and as a consequence the total current increased.

5. CONCLUSIONS

High brightness electron extraction has been obtained from Al, Zn and Cu targets illumined by a XeCl and a KrCl laser. The measured output current densities are much larger than that theoretically calculated by EGUN simulation code. The maximum current density extracted in this work was 32 A/cm^2 from Cu target on respect of 6.4 A/cm^2 provided by code. The highest brightness was 0. 64 10^9 A[π m rad]$^{-2}$, from Al target and KrCl laser irradiation. The large discrepancy between the experimental result and the theoretical calculation has been

found also by other authors [5] and we considered to be due to the plasma formation on the sample surface.

With our experimental set-up we have compared the brightness from different cathodes but it is possible, by means of electro-magnetic lens, to improve further the brightness values.

Acknowledgement

The authors would like to acknowledge Dr. V. Stagno for computer simulations.

REFERENCES:

[1] D.W. Feldmann, S.C. Bender, B.E. Carlsten, J. Early, R.B. Feldman, W. Joel, D. Johnson, A.H. Lumpkin, P.G. O'Shea, WE. Stein, R.L.Sheffield, and L.M. Young,"Experimental Results from the Los Alamos FEL Photoinjector" IEEE Quantum Electron. QE-**27**, (1991) 2636

[2] V. Nassisi,"Electron Generation from a Metal Target Induced by an XeCl Laser" Nucl. Instr. Meth. A**340**, (1994) 182

[3] D. Charalambidis, E. Hontzopoulos C. F Fotakis, G. Farkas and C. Toth, "High Current, Small Divergence Electron Beams Produced by Laser-Induced surface Photoelectric Effect" J. Appl. Phys.**65,** (1989) 2843

[4] A. Beloglazov, M. Castellano, M.S. Causo, V. Nassisi and P. Patteri, proceeding of the CLEO 94, IEEE Cat. n. 94TH0614-8, p.147 (1994)

[5] V. Nassisi and A. Pecoraro,"Electron Emissiosn from a Metal Target irradiated by a Excimer Laser" Nucl. Instr. Meth. A**341** (1994) ABS 137

[6] Y. Kawamura, K. Toyoda and M. Kawai," Generation of Relativistic Photoelectrons Induced by an Ultraviolet Laser and Their Propagation Characteristics in a Longitudinal Guiding Magnetic Field", J. Appl. Phys. **71**, (1992) 2507

[7] M.S. Causo, M. Martino and V. Nassisi," Photoelectron-Beam Generation up to Short Thresold" Appl. Phys.B **58** ,(1994) 19

[8] V. Nassisi and V. Stagno," Experimental study of electron generation induced by a XeCl laser" J. Appl. Phys. **76**, (1994) 3769

[9] J.T. Lin and T.F. George, "Laser generated electron emission from surfaces: Effect of the pulse shape on temperature and transient phenomena" J. Appl. Phys. **54** (1983) 382

[10] W. Namkung and E.P. Chojnacki " Emittance measurements of space-charge dominated electron beams" Rev. Sci. Instrum. **57** (1986) 341

[11] J.S. Fraser, R.L. Sheffield and E.R. Gray, "A new High - Brightness electron injector for free electron laser driven by RF Linacs" NIM A **250** (1986) 71

[12] V. Nassisi and A. Luches,"Rogowski coil: theory and experimental results" Rev. Sci. Instrum. **50** (1979) 900.

FIGURE CAPTIONS

Fig. 1. Accelerating chamber. T; Target. I; insulator, HV; High voltage, R; Rogowski coil.

Fig. 2. Experimental set-up: A Accelerating chamber, HV Voltage supplier, P Dove prism, L Convergent lens, M Flat mirror, B beamsplitter, Ph photodiode, F Neutral density filters, RP Root pump, TP Turbo-molecular pump.

Fig. 3: (a) Waveforms of XeCl laser pulse and (b) Rogowski coil and Faraday cup responses from Al target with 5.6 mJ XeCl laser at 20 kV of accelerating voltage.

Fig 4. Current and emittance values of the photoextracted electrons from Al target vs. the accelerating voltage, the pulse energy was 5.6 mJ and the active mixture was XeCl.

Fig. 5. Electron trajectories and equipotential surfaces computed by EGUN simulation code.

Fig. 6. (a) Waveforms of KrCl laser pulse (b) Rogowski coil and Faraday cup response from Al target with the 3.8 mJ KrCl laser at 20 kV of accelerating voltage.

Fig 7. Current and emittance values of the photoextracted electrons from Al target vs. the accelerating voltage, the laser energy was 3.8 mJ and the active mixture was KrCl.

Fig 8 Current and emittance values of the photoextracted electrons from Al target vs. the accelerating voltage, the pulse energy is 0.6 mJ and the active mixture was KrCl.

Fig.9. Total current and emittance values of the photoextracted electrons from Zn target vs the accelerating voltage. The pulse energy was 5.6 mJ and the active mixture was XeCl.

Fig.10. Total current and emittance values of the photoextracted electrons from Zn target vs the accelerating voltage. The pulse energy was 5.6 mJ and the active mixture was KrCl.

Fig.11. Total current and emittance values of the photoextracted electrons from Zn target vs the accelerating voltage. The pulse energy was 0.38 mJ and the active mixture was KrCl.

Fig.12. Total current and emittance values of the photoextracted electrons from Cu target vs the accelerating voltage. The pulse energy was 5.6 mJ and the active mixture was XeCl.

Fig.13. Total current emittance values of the photoextracted electrons from Cu target vs the accelerating voltage. The pulse energy was 5.6 mJ and the active mixture was KrCl.

Fig.14. Total current emittance values of the photoextracted electrons from Cu target vs the accelerating voltage. The pulse energy was 1 mJ and the active mixture was KrCl.

Fig.15. Output current from Al target at anode-cathode gap 2 mm.

Fig. 16. Output current from Al target at anode-cathode gap 16 mm.

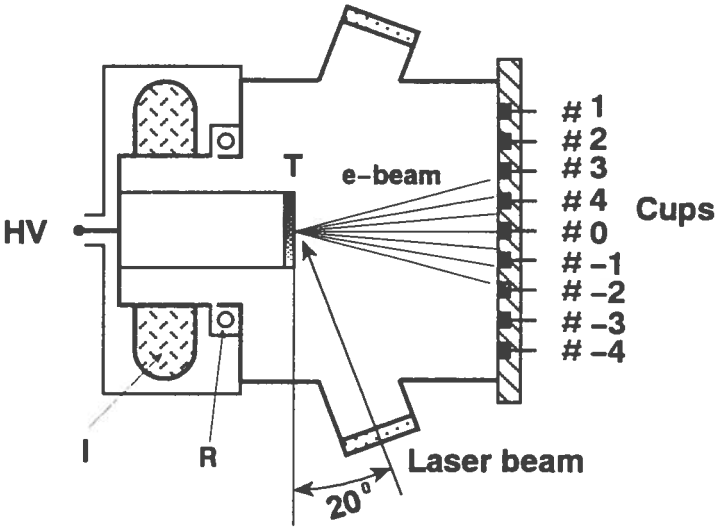
HV
T
e-beam
1
2
3
4
0
-1
-2
-3
-4
Cups
I
R
Laser beam
20°

Fig. 1

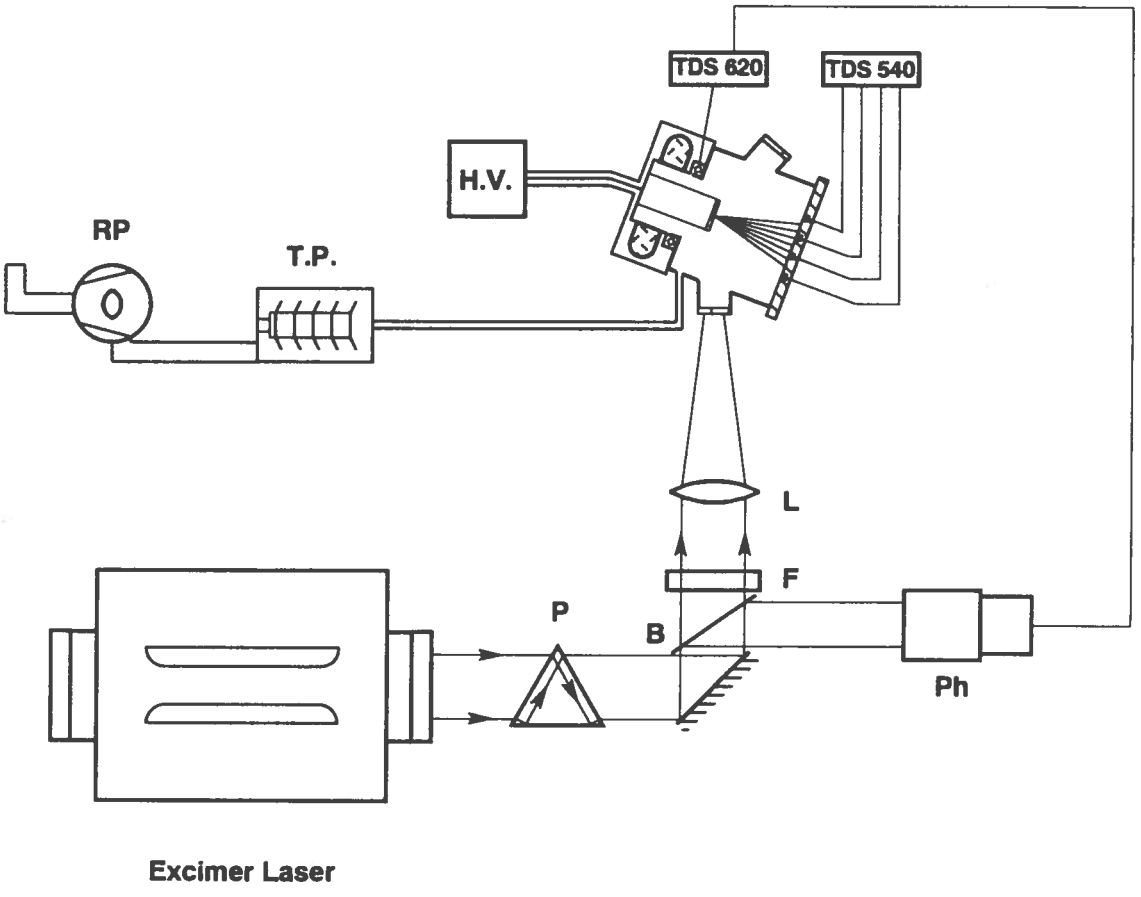
TDS 620
TDS 540
H.V.
RP
T.P.
L
F
P
B
Ph
Excimer Laser

Fig. 2

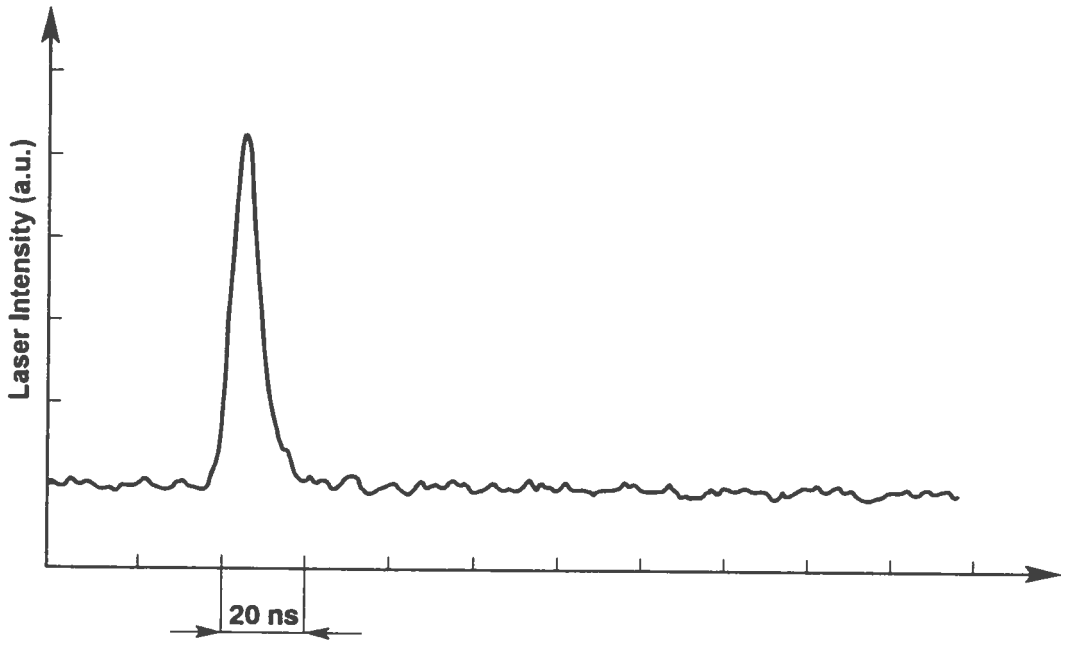
Laser Intensity (a.u.)
20 ns

Fig. 3a

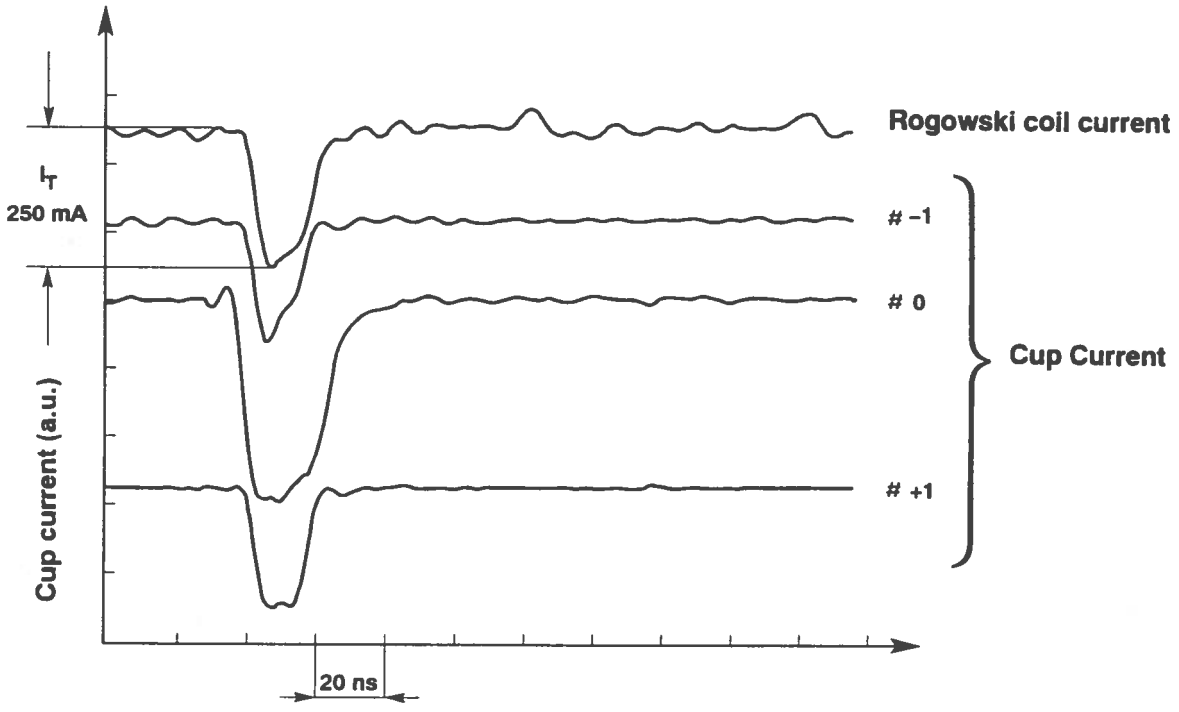
Rogowski coil current
I_T
250 mA
-1
0
Cup Current
+1
Cup current (a.u.)
20 ns

Fig. 3b

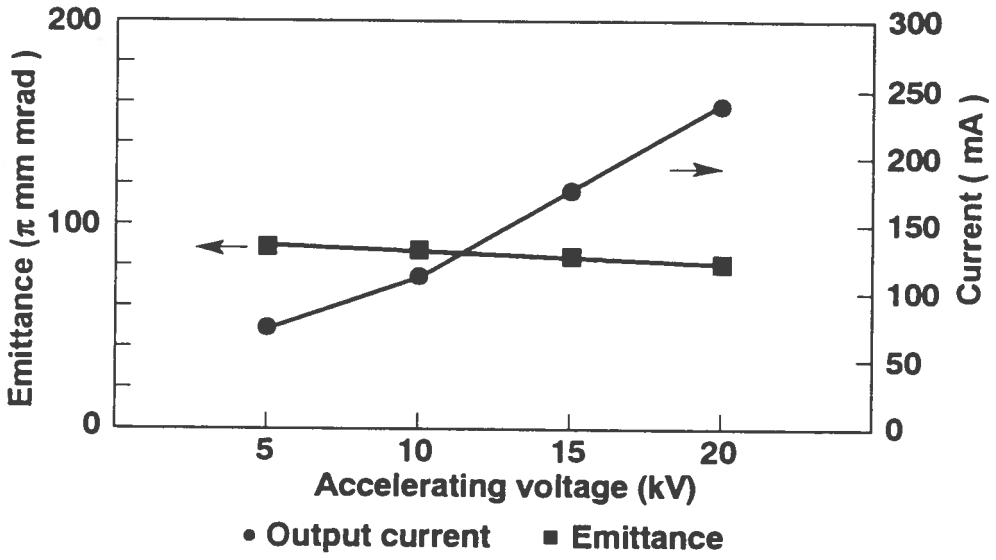
200
100
0
Emittance (π mm mrad)
300
250
200
150
100
50
0
Current (mA)
5
10
15
20
Accelerating voltage (kV)
• Output current
■ Emittance

Fig. 4

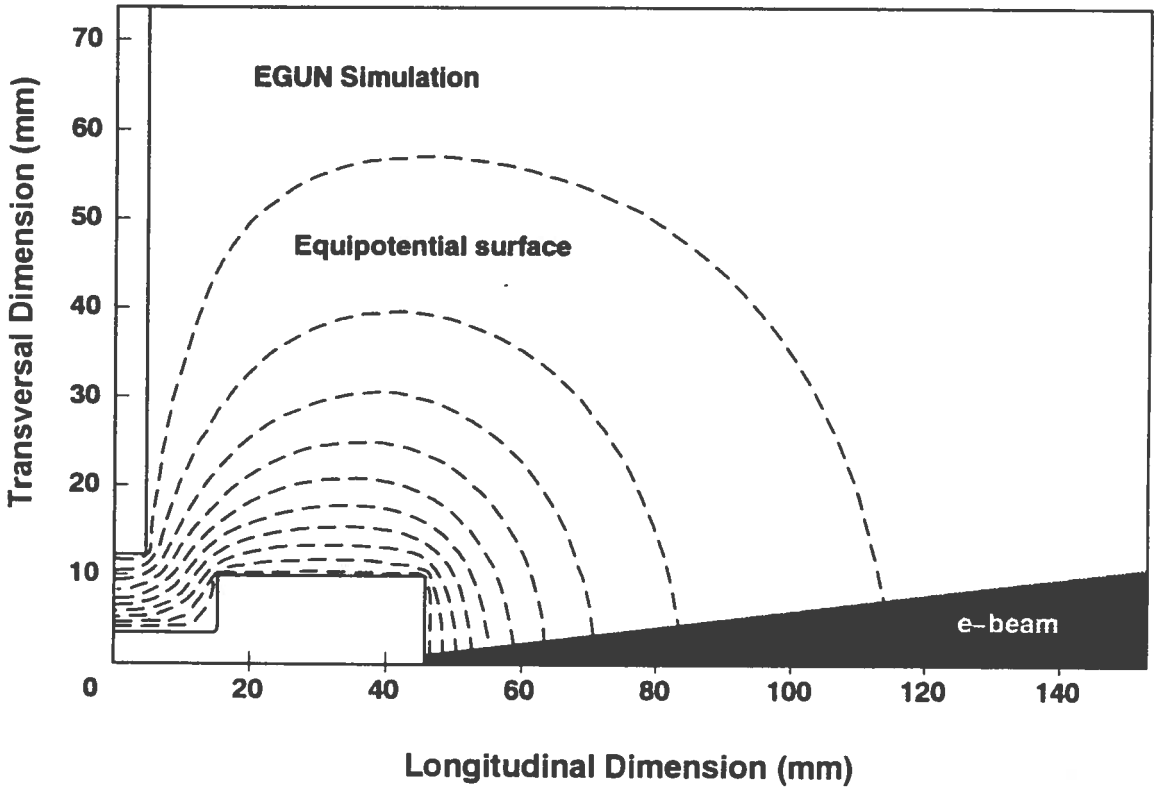
EGUN Simulation
Equipotential surface
e-beam
Transversal Dimension (mm)
70
60
50
40
30
20
10
0
20
40
60
80
100
120
140
Longitudinal Dimension (mm)

Fig. 5

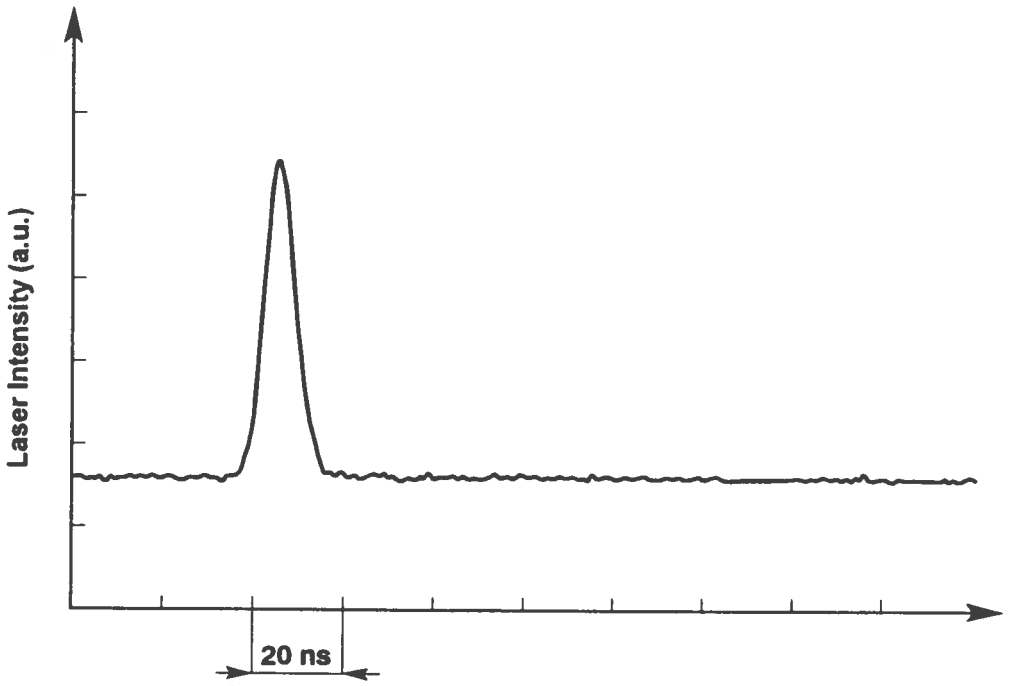
Laser Intensity (a.u.)
20 ns

Fig. 6a

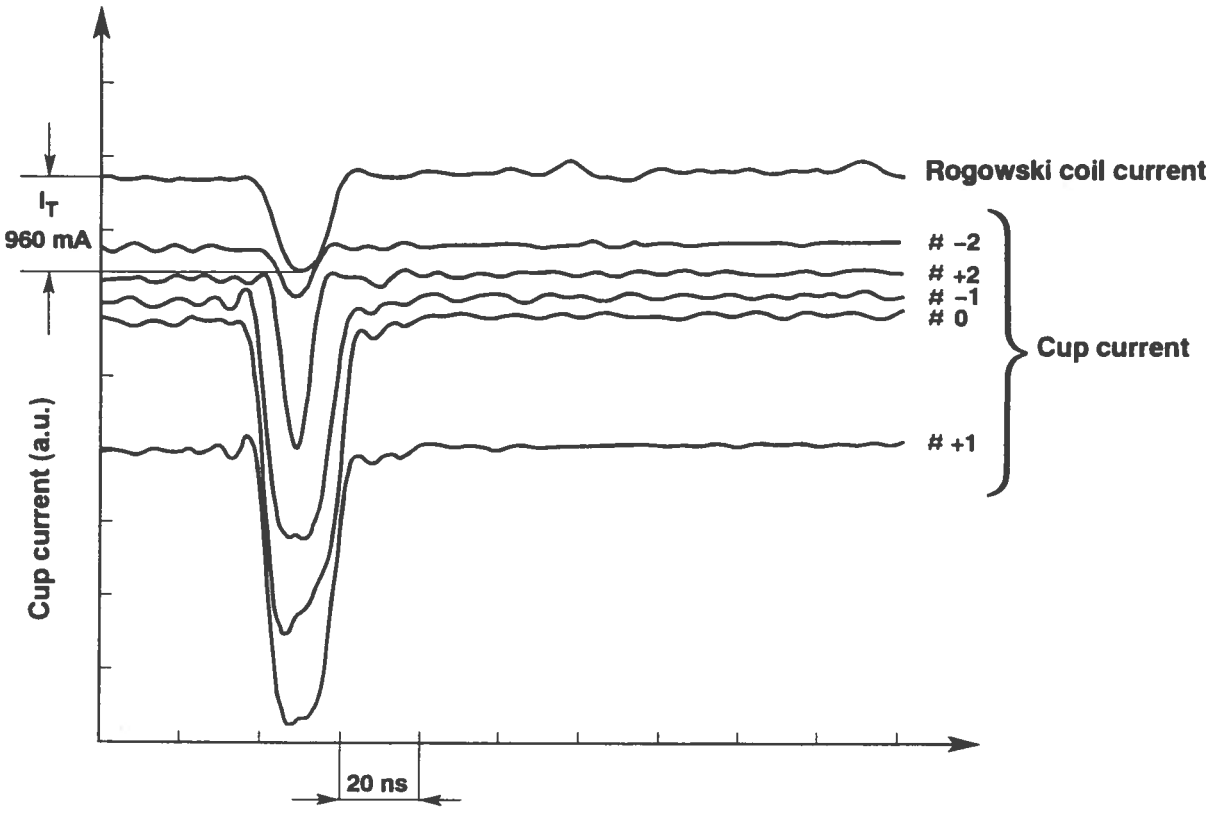
Rogowski coil current
I_T
960 mA
−2
+2
−1
0
Cup current
+1
Cup current (a.u.)
20 ns

Fig. 6b

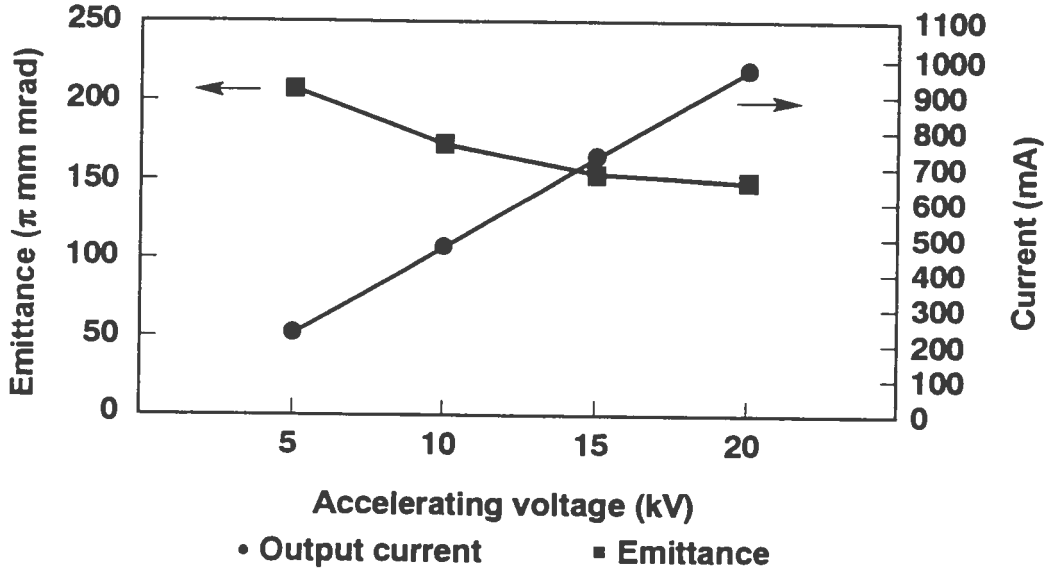
Emittance (π mm mrad)
250
200
150
100
50
0
1100
1000
900
800
700
600
500
400
300
200
100
0
Current (mA)
5
10
15
20
Accelerating voltage (kV)
• Output current
▪ Emittance

Fig. 7

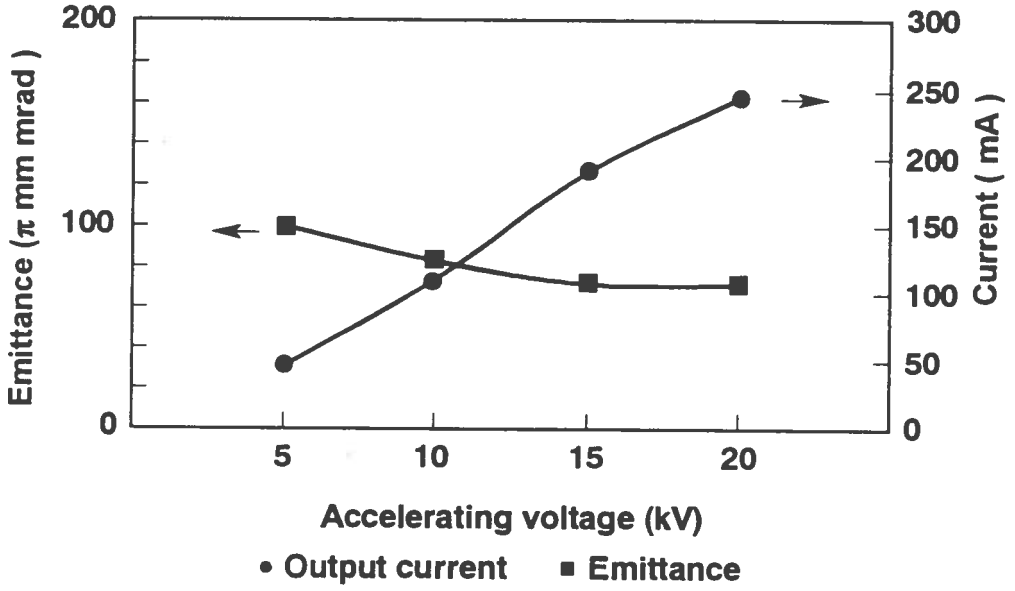
Emittance (π mm mrad)
200
100
0
300
250
200
150
100
50
0
Current (mA)
5
10
15
20
Accelerating voltage (kV)
• Output current
▪ Emittance

Fig. 8

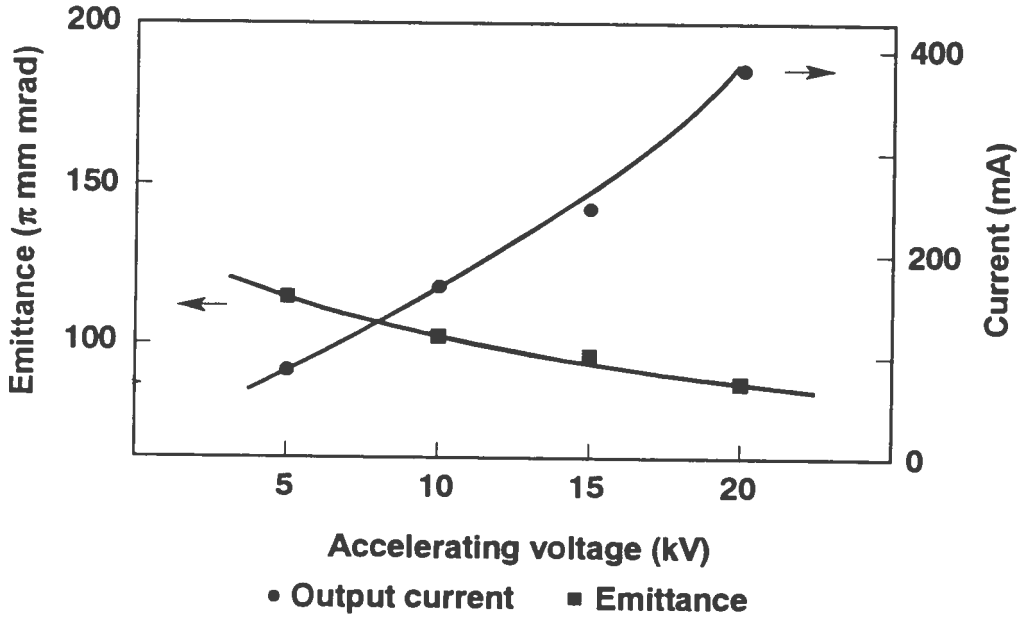
200
150
100
Emittance (π mm mrad)
400
200
0
Current (mA)
5
10
15
20
Accelerating voltage (kV)
• Output current
■ Emittance

Fig. 9

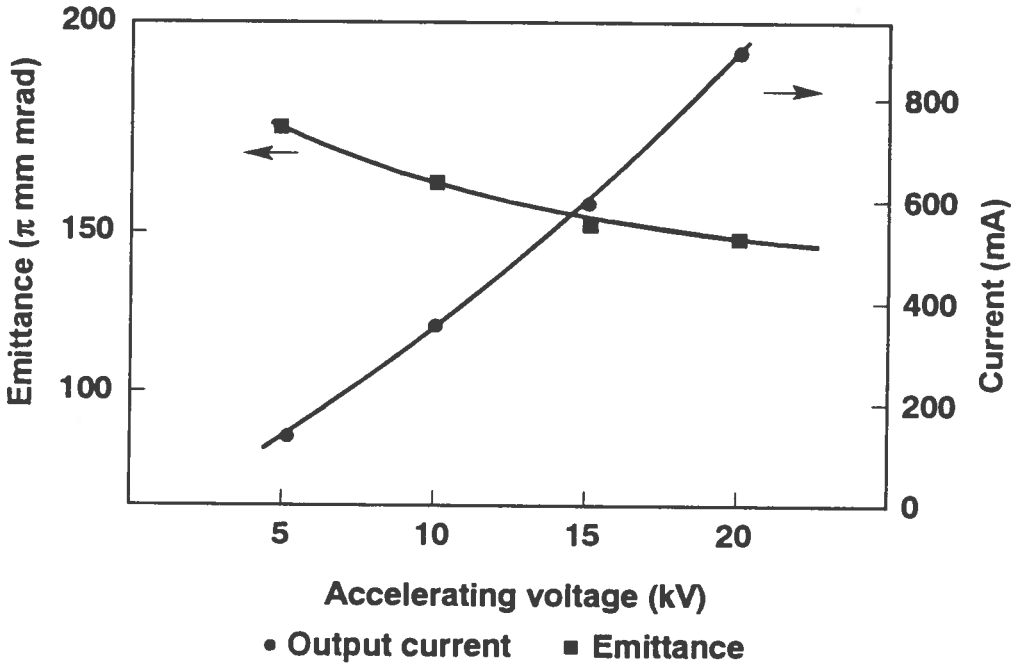
200
150
100
Emittance (π mm mrad)
800
600
400
200
0
Current (mA)
5
10
15
20
Accelerating voltage (kV)
• Output current
■ Emittance

Fig. 10

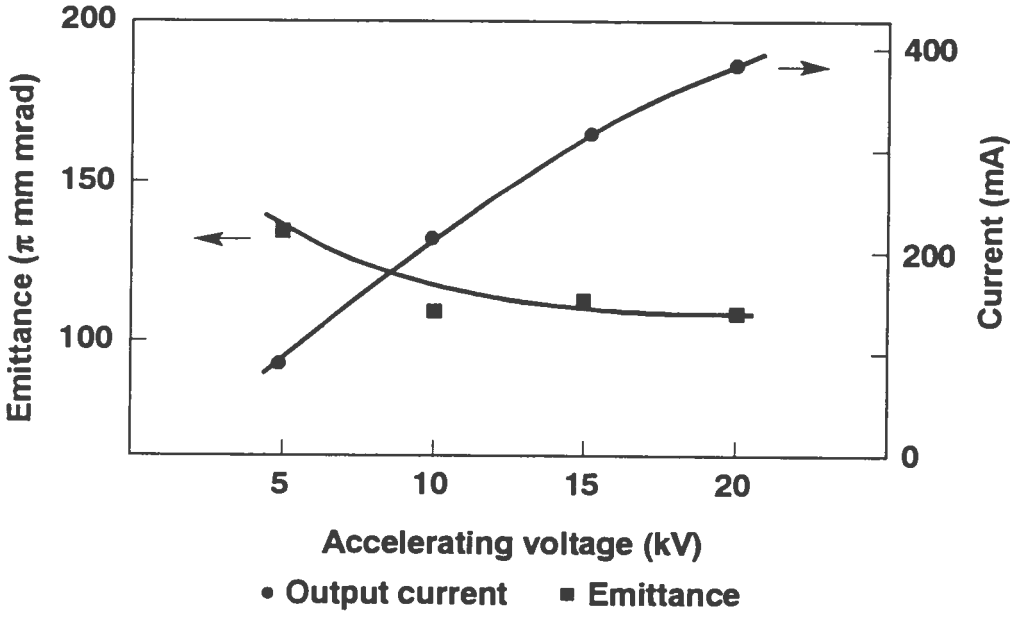
200
150
100
Emittance (π mm mrad)
400
200
0
Current (mA)
5
10
15
20
Accelerating voltage (kV)
• Output current
■ Emittance

Fig. 11

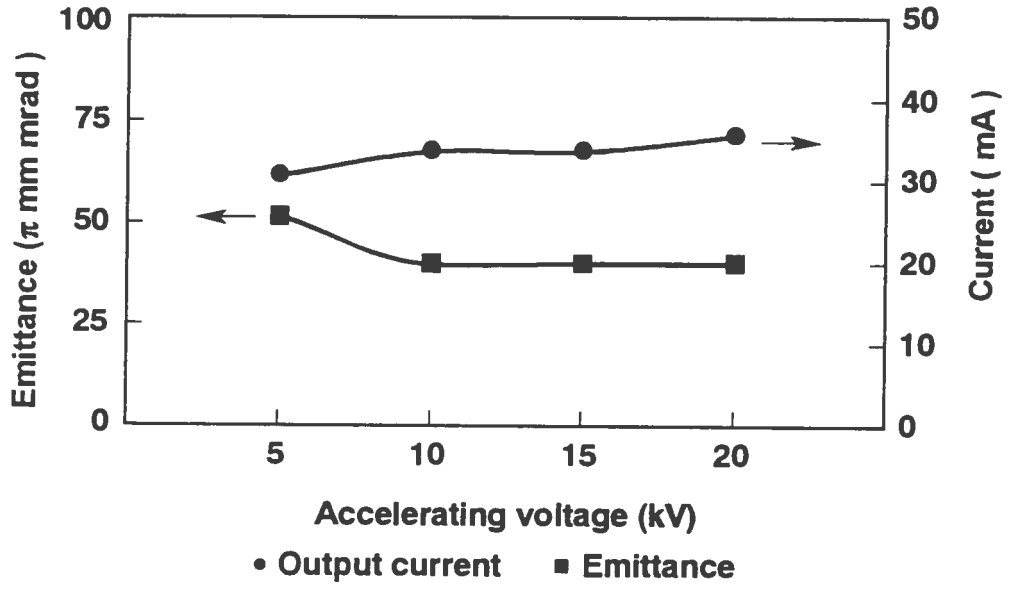
100
75
50
25
0
Emittance (π mm mrad)
50
40
30
20
10
0
Current (mA)
5
10
15
20
Accelerating voltage (kV)
• Output current
■ Emittance

Fig. 12

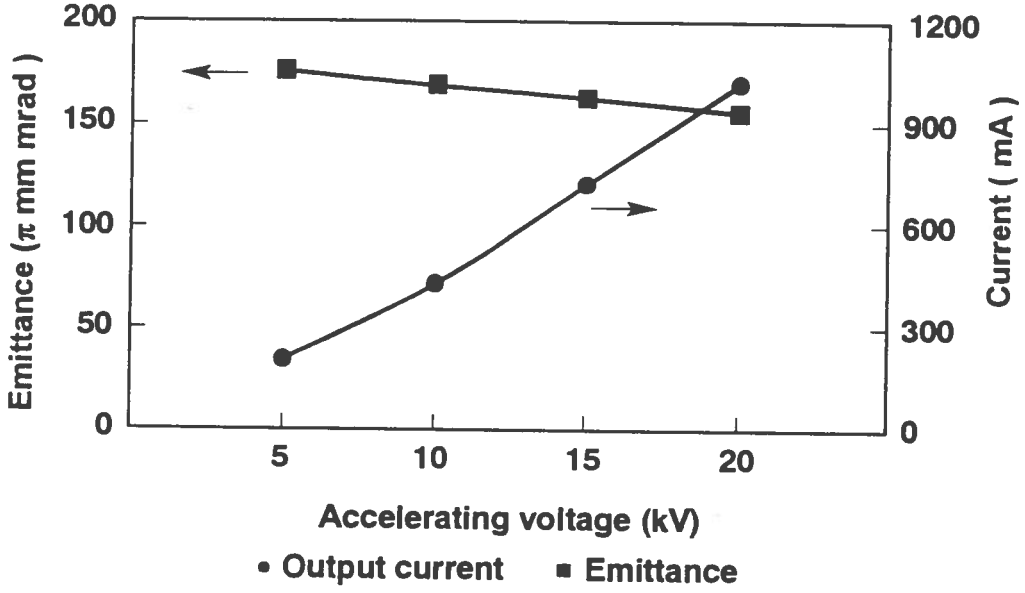
200
150
100
50
0
Emittance (π mm mrad)
1200
900
600
300
0
Current (mA)
5
10
15
20
Accelerating voltage (kV)
• Output current
■ Emittance

Fig. 13

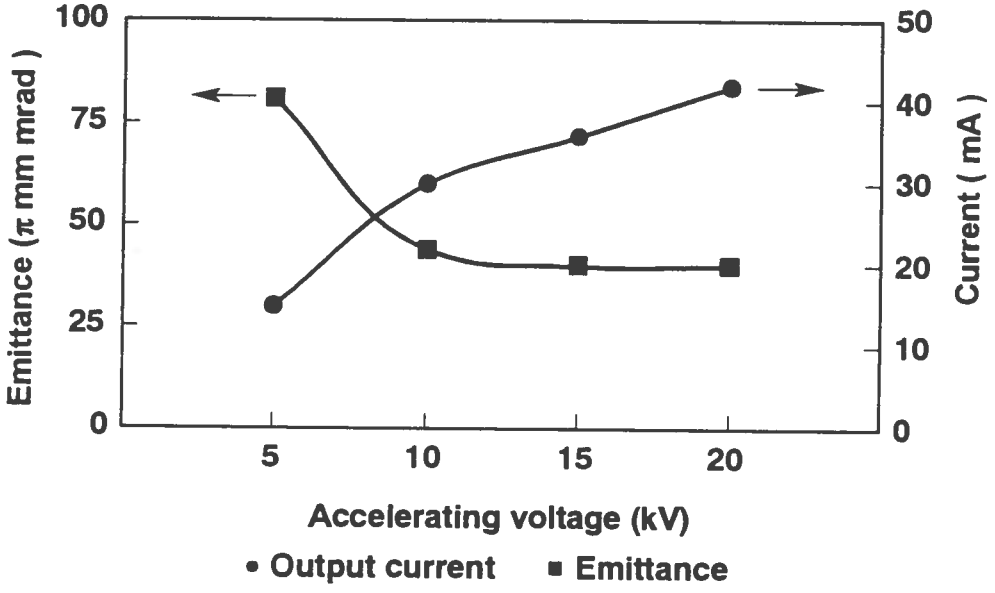
100
75
50
25
0
Emittance (π mm mrad)
50
40
30
20
10
0
Current (mA)
5
10
15
20
Accelerating voltage (kV)
• Output current
■ Emittance

Fig. 14

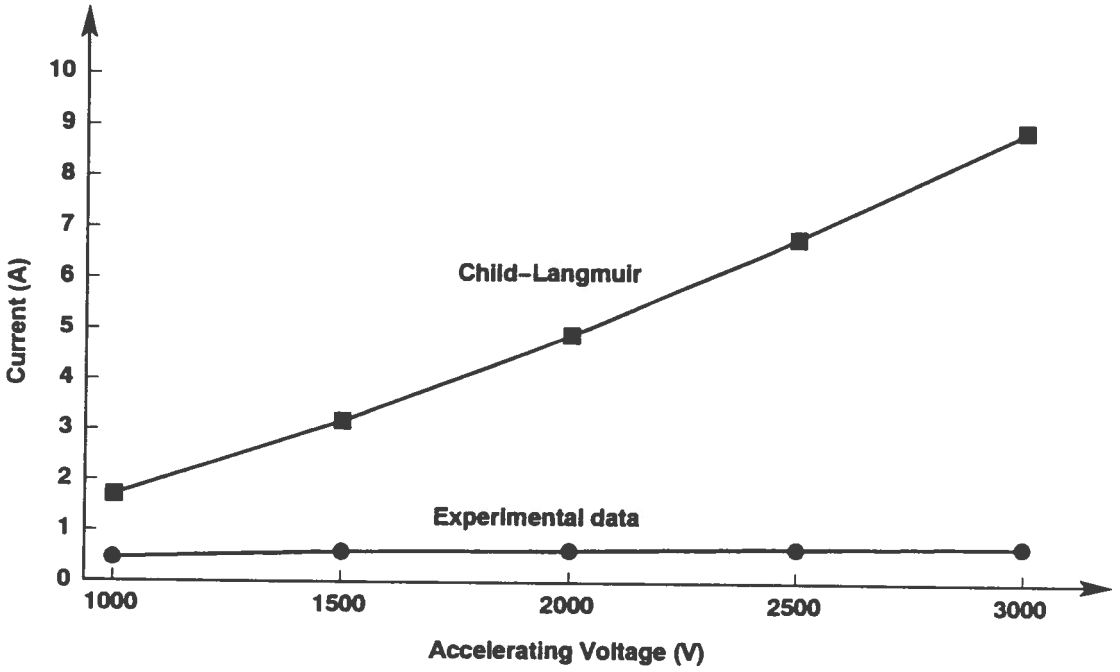
Current (A)
10
9
8
7
6
5
4
3
2
1
0
Child–Langmuir
Experimental data
1000
1500
2000
2500
3000
Accelerating Voltage (V)

Fig. 15

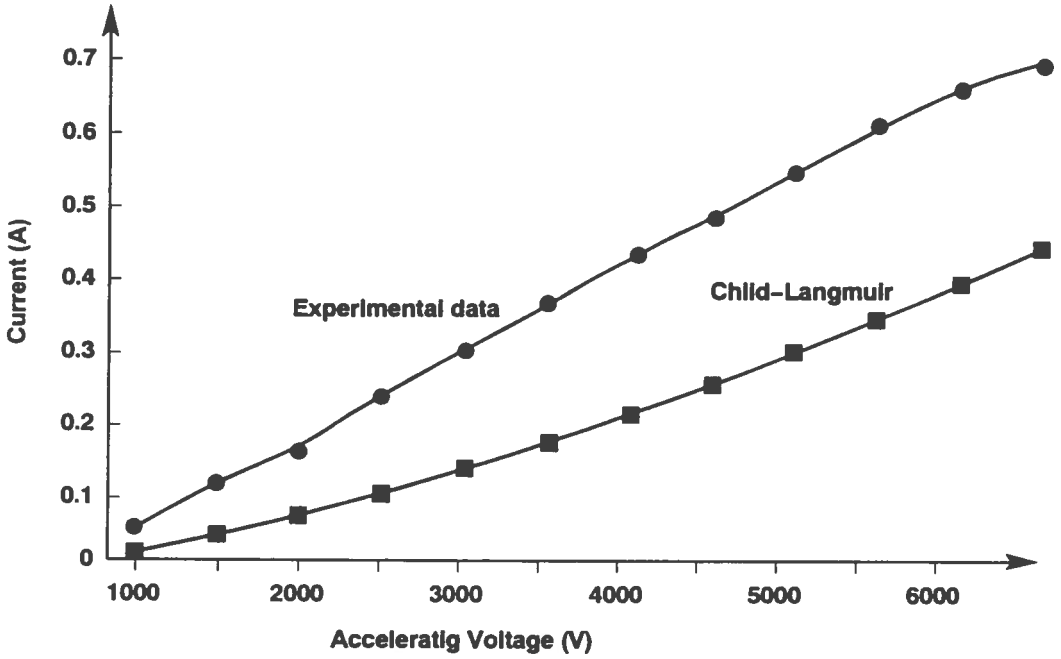
Current (A)
0.7
0.6
0.5
0.4
0.3
0.2
0.1
0
Experimental data
Child–Langmuir
1000
2000
3000
4000
5000
6000
Acceleratig Voltage (V)

Fig. 16